

# Josephson current in nanofabricated V/Cu/V mesoscopic junctions

César Pascual García<sup>1,\*</sup> and Francesco Giazotto<sup>1,†</sup>

<sup>1</sup>NEST CNR-INFM and Scuola Normale Superiore, Piazza dei Cavalieri 7, I-56126 Pisa, Italy

(Dated: October 30, 2018)

We report the fabrication of planar V/Cu/V mesoscopic Josephson weak-links of different size, and the analysis of their low-temperature behavior. The shorter junctions exhibit critical currents of several tens of  $\mu\text{A}$  at 350 mK, while Josephson coupling persists up to  $\sim 2.7$  K. Good agreement is obtained by comparing the measured switching currents to a model which holds in the diffusive regime. Our results demonstrate that V is an excellent candidate for the implementation of superconducting nanodevices operating at a few Kelvin.

PACS numbers: 74.78.Na, 74.50.+r, 74.45.+c

Josephson coupling in superconductor-normal metal-superconductor (SNS) proximity junctions is one of the key manifestations of quantum coherence in mesoscopic systems [1, 2, 3, 4]. For this reason it has been attracting a lot of interest from both the fundamental and the applied physics point of view [5]. Most of *metallic* SNS weak-links are realized within the diffusive regime, and belong typically to the *long*-junction limit which holds for  $\Delta \gg E_{Th}$ . Here  $\Delta$  is the superconducting order parameter,  $E_{Th} = \hbar D/L^2$  is the Thouless energy,  $D$  is the diffusion coefficient of the N region, and  $L$  its length. In such a limit,  $E_{Th}$  sets the zero-temperature critical current of the junction [6], as well as it determines the scale of supercurrent decay with temperature ( $T$ ) for  $k_B T \gg E_{Th}$  [6, 7], where  $k_B$  is the Boltzmann constant. Yet, when the temperature is such that  $\Delta(T)$  becomes comparable to  $E_{Th}$ , both these energies turn out to be relevant to control the junction response. Therefore, larger Thouless energy as well as enhanced  $\Delta$  are required to extend the operation of the SNS junction at higher temperatures. While the former issue can be solved by shortening  $L$ , the latter requires the exploitation of S materials with higher critical temperature ( $T_c$ ). So far, most of nanofabricated planar SNS junctions make a widespread use of aluminum [2, 3, 4, 8, 9, 10, 11], which limits operation below  $T \sim 1.2$  K, or niobium ( $T_c \simeq 9.2$  K) [1, 6, 8, 9, 12] that, however, requires more complex fabrication protocols owing to its high melting point [1, 8, 13]. On the other hand, among elemental superconductors, vanadium (V) has a number of attractive features. It is a group-V transition metal like Nb and Ta, and its bulk  $T_c \simeq 5.4$  K [14] allows applications around liquid  $^4\text{He}$  temperatures. Furthermore, its melting point is low enough to allow evaporation with ease. These characteristics make in principle V suitable for the implementation of superconducting circuits operating at temperatures accessible with the technology of  $^4\text{He}$  cryostats.

In this Letter we report the fabrication of planar V/Cu/V mesoscopic Josephson weak-links, and their characterization down to  $T \sim 350$  mK. The samples exhibit sizeable critical currents whose behavior follows what expected in the long-junction limit. The ease of

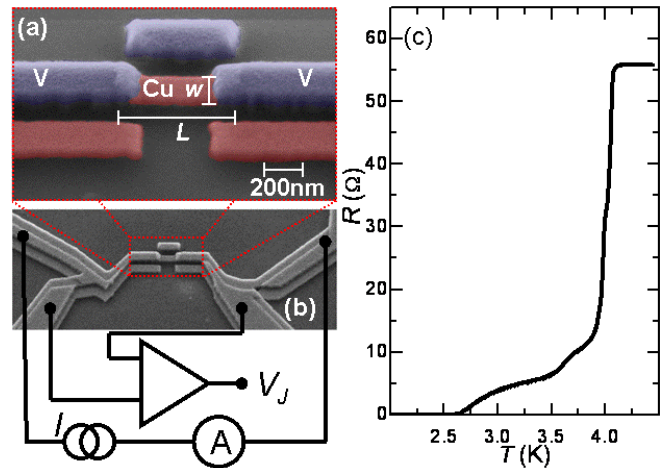


FIG. 1: (Color online) (a) Scanning electron micrograph showing the blow-up of a V/Cu/V weak-link in a typical device (sample B). (b) Sketch of the measurement setup. (c) Zero-bias resistance vs temperature for sample A.

fabrication combined with the quality of the structures make the V/Cu material system relevant for the realization of superconducting nanodevices.

Samples were fabricated by electron beam lithography and two-angle shadow-mask evaporation onto an oxidized Si substrate. A 5-nm-thick Ti layer was first evaporated to improve the adhesion of the metallic films to the substrate. The N region of the weak-link consists of a 40-nm-thick Cu island whose total length  $L$  and width ( $w$ ), depending on the sample, is within the range  $\sim 420 \dots 780$  nm, and  $\sim 45 \dots 190$  nm, respectively. From the normal-state resistance of the junctions ( $R_N$ ) we extracted the Cu diffusion coefficient which lies in the range  $D \sim 74 \dots 130$   $\text{cm}^2/\text{s}$  for the four samples. Vanadium was evaporated as the last step at a high deposition rate (10  $\text{\AA}/\text{s}$ ) to avoid oxygen contamination which can lower its critical temperature [15]. The thickness of the V film was 120 nm for all samples, and was optimized in order to maximize  $T_c$ . The main parameters of the four samples are summarized in Table I. The

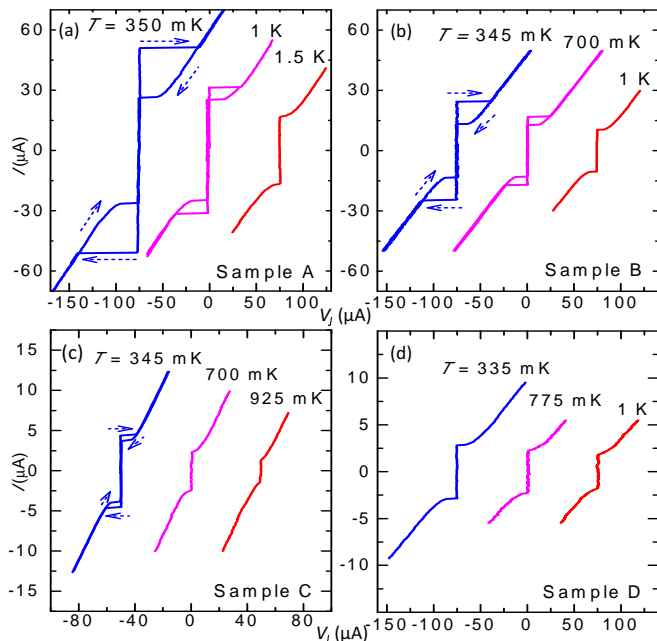


FIG. 2: (Color online) Current vs voltage characteristics of all samples at three different representative temperatures. The curves are horizontally offset for clarity.

junctions were characterized down to  $T \simeq 330$  mK in a filtered  $^3\text{He}$  cryostat.

Figure 1 (a) displays the blow-up of a typical V/Cu/V weak-link (sample B). The V leads overlap the Cu island laterally for  $\sim 100$  nm in all the samples. A micrograph of the same device along with a scheme of the measurement setup used for the characterization is shown in Fig. 1(b). It can be noted the presence of sample portions consisting of Ti/V and Ti/Cu/V layers nearby the junction. Figure 1(c) shows the zero-bias differential resistance ( $R$ ) vs bath temperature for sample A. Above  $T = 4.2$  K the resistance corresponds to that of the whole device in the normal state, while the first transition occurring at  $T \simeq 4.1$  K sets the critical temperature of

TABLE I: Samples parameters. The junctions total length ( $L$ ), width ( $w$ ), and normal-state resistance ( $R_N$ ) are shown. The experimental Thouless energy ( $E_{Th}^{Exp}$ ) is determined from  $R_N$  and the samples geometrical dimensions [17]. The superconducting gap is  $\Delta \simeq 0.62$  meV for all samples.  $E_{Th}^{Fit}$  and the suppression coefficient  $\alpha$  are fit parameters of Fig. 3. (see text).

Sample	$L$ (nm)	$w$ (nm)	$R_N$ ( $\Omega$ )	$E_{Th}^{Exp}$ ( $\mu\text{eV}$ )	$\Delta/E_{Th}^{Exp}$	$E_{Th}^{Fit}$ ( $\mu\text{eV}$ )	$\alpha$
A	420	184	1.55	34.3	18.1	36.0	0.38
B	636	189	1.62	21.1	29.5	20.3	0.36
C	783	172	2.86	10.6	58.4	10.4	0.34
D	430	46	7.80	26.6	23.4	32.7	0.125

the V film. From the latter we deduced a superconducting energy gap  $\Delta = 1.764k_B T_c \simeq 0.62$  meV [16]. The double transition, occurring around 3.7 K and 3 K, can be ascribed to the critical temperatures of the metallic bilayer and triple-layer present in the structures [see Fig. 1(b)]. Then, below  $T \simeq 2.75$  K, the zero-bias resistance drops to zero indicating that the junction is in the Josephson regime, and an observable supercurrent is established. The four samples exhibited a very similar behavior, apart from the transition temperature to the supercurrent state.

Figure 2 shows the current-voltage ( $I$  vs  $V_J$ ) characteristics of all the samples at three different representative temperatures. The curves are horizontally offset for clarity. In particular, for sample A at  $T = 350$  mK [see panel (a)] the  $I$  vs  $V_J$  displays a clear Josephson effect with a switching current  $I_s = 52 \mu\text{A}$ . It also shows a marked hysterical behavior, i.e., once the weak-link has switched to the resistive state it recovers the dissipationless regime at a much smaller bias current, i.e., the retrapping current ( $I_r$ ). In sample A,  $I_r = 27 \mu\text{A}$  at  $T = 350$  mK. The origin of hysteresis in mesoscopic Josephson junctions with large critical current has been recently investigated by Courtois *et al.* [4], and stems from electron heating in the N region once the junction switches to the dissipative branch. Furthermore, the hysteresis decreases at higher bath temperature, and disappears around  $T = 1.5$  K. Notably, sample A obtains  $I_s = 17 \mu\text{A}$  at  $T = 1.5$  K. A similar general behavior is also observed for the current-voltage characteristics of sample B, shown in Fig. 2(b). The switching current is lower in this case due to the increased length of the N wire, and also its hysterical behavior is less pronounced. Following the same trend, the current-voltage characteristics of sample C [see Fig. 2(c)] show a lower  $I_s$ , and a much reduced hysteresis has been observed only at the lowest temperatures. In sample D, the N-region length is similar to that of sample A but its width is narrower which results in a higher  $R_N$ . The switching current is therefore lower, and the hysteresis is nearly absent at all the investigated temperatures [see Fig. 2(d)].

The impact of the N-region size on the supercurrent is displayed in Fig. 3 which summarizes the results obtained in all four devices. Full dots and open squares represent the  $I_s$ 's and  $I_r$ 's, respectively, extracted from the junctions current-voltage characteristics taken at different temperatures. The decay of  $I_s$  and the softening of the hysteresis with  $T$  is evident. As explained above, the switching current and the hysteresis are larger for sample A [Fig. 3(a)], and decrease as  $R_N$  increases. As expected [6, 7], the decay of  $I_s$  with temperature is also faster for longer junctions (sample B and C), i.e., those with a lower  $E_{Th}$  [see Fig. 3(b) and (c)]. Meanwhile sample D shows almost no hysteresis, and its supercurrent is less affected by the temperature than samples B and C as expected from its higher  $E_{Th}$  [Fig. 3(d)]. Furthermore,  $I_r$

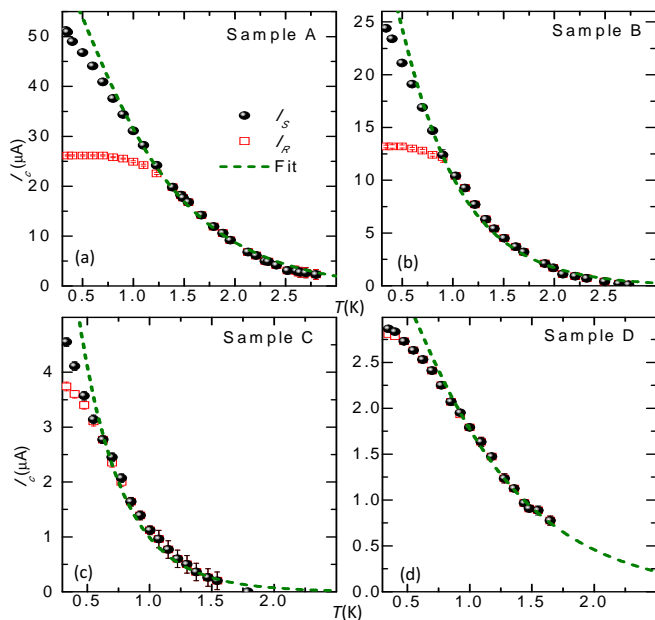


FIG. 3: (Color online) Critical current  $I_c$  vs  $T$  for all four devices. Full dots and dashed lines represent the switching current ( $I_s$ ) and the high-temperature fit, respectively. The retrapping current ( $I_r$ ) is also shown as open squares.

saturates below a threshold temperature which is higher for junctions with larger  $I_s$ . We remark the persistence of the Josephson coupling in all samples up to high  $T$  (in sample A, for instance,  $I_s$  is clearly observable up to  $T \simeq 2.7$  K). This points up the advantage of using V as superconductor to extend the junctions operation at higher temperatures.

The examination of Table I shows that  $\Delta/E_{Th}^{Exp} \gg 1$  which provides the frame of the *long*-junction limit. Here  $E_{Th}^{Exp}$  is the experimental Thouless energy which has been determined from the junctions geometrical dimensions and  $R_N$  [17]. In order to make a more quantitative analysis of the data we recall that the critical current of a long diffusive Josephson junction in the high-temperature regime ( $k_B T \gtrsim 5E_{Th}$ ) is given by [6, 7]

$$I_s(T) = \frac{64\pi k_B T}{eR_N} \sum_{n=0}^{\infty} \frac{\sqrt{\frac{2\omega_n}{E_{Th}} \Delta^2(T) \exp[-\sqrt{\frac{2\omega_n}{E_{Th}}}]}}{[\omega_n + \Omega_n + \sqrt{2(\Omega_n^2 + \omega_n \Omega_n)}]^2}, \quad (1)$$

where  $\omega_n(T) = (2n + 1)\pi k_B T$ , and  $\Omega_n(T) = \sqrt{\Delta^2(T) + \omega_n^2(T)}$ . Dashed lines in Fig. 3 represent the best fit to the data calculated from Eq. (1) by setting the nominal  $R_N$  and  $\Delta$  values, and using as fitting parameters the Thouless energy ( $E_{Th}^{Fit}$ ) and a suppression coefficient ( $\alpha$ ) [4] multiplying Eq. (1) which accounts for nonideality of the junction. For  $\Delta(T)$  we used the usual BCS temperature dependence of the gap. For all devices good agreement with the data is obtained by setting  $E_{Th}^{Fit}$  very close to the experimental estimate with  $\alpha \sim 0.35$  for the first three samples (A-C), and  $\alpha = 0.125$  for sample

D (see Table I). The origin of  $I_s$  suppression [4, 8, 11] is at present not fully understood, but such values for  $\alpha$  [4] may suggest the presence of enhanced scattering due to disorder in the junction, or at the SN interface which could be intrinsic to the nature of V/Cu metallurgical contact. As suggested by M. Yu. Kupriyanov [18] a plausible reason for this suppression stems from the overlapped geometry typical of shadow-mask evaporated structures, which leads to a more complex system than the SNS one described by Eq. (1), in particular at both NS boundaries which consist of layered proximized regions. We note finally that this deviation from theoretical prediction of Eq. (1) is not to be ascribed to quasiparticle overheating in the N region, due to the strong electron-acoustic phonon coupling in such a high temperature regime [19].

In conclusion, we have reported the fabrication of V/Cu/V proximity Josephson junctions, and their characterization at cryogenic temperatures. The weak-links are easy to fabricate with present-day technology, and show sizeable critical currents at temperatures of a few Kelvin. The supercurrents decay with temperature is in good agreement with what expected in the diffusive regime, while their amplitude shows a reduction which could be related to the nature of the V/Cu contact. Our results demonstrate that V/Cu/V mesoscopic junctions are an attractive choice for the implementation of a broad range of superconducting devices, for instance, from SQUIDS [3, 5, 8] and out-of-equilibrium Josephson transistors [1, 10, 11, 12, 19] to radiation sensors [20].

We acknowledge T. T. Hekkilä, J. P. Pekola, and F. Taddei for fruitful discussions, M. Yu. Kupriyanov for pointing out a possible mechanism for supercurrent suppression in our Josephson junctions, and partial financial support from the NanoSciERA "NanoFridge" project.

\* Electronic address: c.pascual@sns.it

† Electronic address: f.giazotto@sns.it

- [1] J. J. A. Baselmans, A. F. Morpurgo, B. J. van Wees, and T. M. Klapwijk, *Nature (London)* **397**, 43 (1999).
- [2] Y.-J. Doh, J. A. van Dam, A. L. Roest, E. P. A. M. Bakkers, L. P. Kouwenhoven, and S. De Franceschi, *Science* **309**, 272 (2005).
- [3] H. le Sueur, P. Joyez, H. Pothier, C. Urbina, and D. Esteve, *Phys. Rev. Lett.* **100**, 197002 (2008).
- [4] H. Courtois, M. Meschke, J. T. Peltonen, and J. P. Pekola, *Phys. Rev. Lett.* **101**, 067002 (2008).
- [5] K. K. Likharev, *Dynamics of Josephson Junctions and Circuits* (Gordon and Breach, New York, 1991).
- [6] P. Dubos, H. Courtois, B. Pannetier, F. K. Wilhelm, A. D. Zaikin, and G. Schön, *Phys. Rev. B* **63**, 064502 (2001).
- [7] A. D. Zaikin and G. F. Zharkov, *Sov. J. Low Temp. Phys.* **7**, 184 (1981).
- [8] L. Angers, F. Chiodi, G. Montambaux, M. Ferrier, S. Gueron, H. Bouchiat, and J. C. Cuevas, *Phys. Rev. B*

- 77**, 165408 (2008).
- [9] T. Hoss, C. Strunk, T. Nussbaumer, R. Huber, U. Staufer, and C. Schönenberger, *Phys. Rev. B* **62**, 4079 (2000).
- [10] M. S. Crosser, J. Huang, F. Pierre, P. Virtanen, T. T. Heikkilä, F. K. Wilhelm, and N. O. Birge, *Phys. Rev. B* **77**, 014528 (2008).
- [11] A. M. Savin, J. P. Pekola, J. T. Flyktman, A. Anthore, and F. Giazotto, *Appl. Phys. Lett.* **84**, 4179 (2004).
- [12] A. F. Morpurgo, T. M. Klapwijk, and B. J. van Wees, *Appl. Phys. Lett.* **72**, 966 (1998).
- [13] P. Dubos, P. Charlat, Th. Crozes, P. Paniez, and B. Panetier, *J. Vac. Sci. Technol. B* **18**, 122 (2000).
- [14] R. Radebaugh and P. H. Keesom, *Phys. Rev.* **149**, 209 (1966).
- [15] A. Wexler and W. S. Corak, *Phys. Rev.* **85**, 85 (1952).
- [16] R. J. Noer, *Phys. Rev. B* **12**, 4882 (1975).
- [17] We recall that  $D = L/(\nu_F e^2 t w R_N)$  where  $t = 40$  nm is the N island thickness, and  $\nu_F = 1.56 \times 10^{47} \text{ J}^{-1} \text{ m}^{-3}$  is the density of states at the Fermi level of Cu.
- [18] M. Yu. Kupriyanov, private communication.
- [19] F. Giazotto, T. T. Heikkilä, A. Luukanen, A. M. Savin, and J. P. Pekola, *Rev. Mod. Phys.* **78**, 217 (2006).
- [20] F. Giazotto, T. T. Heikkilä, G. P. Pepe, P. Heliö, A. Luukanen, and J. P. Pekola, *Appl. Phys. Lett.* **92**, 162507 (2008).